INFECTION AND IMMUNITY, Nov. 1997, p. 4761–4769 Vol. 65, No. 11
0019-9567/97/$04.00+0

Profiles of Healing and Nonhealing *Cryptosporidium parvum* Infection in C57BL/6 Mice with Functional B and T Lymphocytes: the Extent of Gamma Interferon Modulation Determines the Outcome of Infection

CYNTHIA M. THEODOS,[1]* KRISTEN L. SULLIVAN,[1]† JEFFREY K. GRIFFITHS,[1,2,3] AND SAUL TZIPORI[1,4]

Division of Infectious Diseases, Department of Biomedical Sciences, Tufts University School of Veterinary Medicine, North Grafton, Massachusetts 01536[1]; Department of Family Medicine and Community Health and Department of Medicine, Tufts University School of Medicine,[2] and Division of Geographic Medicine and Infectious Diseases, Tufts-New England Medical Center,[4] Boston, Massachusetts 02111; and Division of Infectious Diseases, St. Elizabeth's Medical Center of Boston, Boston, Massachusetts 02135[3]

Received 6 June 1997/Returned for modification 9 July 1997/Accepted 21 August 1997

This study describes healing and nonhealing models of *Cryptosporidium parvum* infection with adult mice that have functional T and B lymphocytes. In our nonhealing model, mice on a C57BL/6 background which have a targeted disruption in the gamma interferon (IFN-γ) gene (GKO mice) are utilized. *C. parvum*-infected GKO mice shed extremely high levels of oocysts and displayed overwhelming infection of the entire small intestine. The majority of these mice succumbed within 2 to 3 weeks due to severe acute infection and profound mucosal destruction. In our healing murine model, C57BL/6J mice treated with a single injection of the neutralizing anti-IFN-γ monoclonal antibody XMG 1.2 prior to infection were used. These mice developed two peaks of oocyst shedding but were ultimately free of parasites on day 30 of infection. Again, the small intestine was the primary site of infection. Mesenteric lymph node (MLN) cells isolated from *C. parvum*-infected nonhealing GKO mice proliferated and secreted interleukin 2 (IL-2) but not IFN-γ or IL-4 in response to ex vivo restimulation with intact *C. parvum* sporozoites or a *C. parvum* sporozoite antigen preparation. In contrast, parasite-specific MLN cells isolated from healing C57BL/6J mice secreted IL-2 and IFN-γ but not IL-4. These results suggest that IFN-γ, either directly or indirectly, is important for resistance to and resolution of cryptosporidiosis. Moreover, these models now allow the analysis of parasite-specific cell-mediated and humoral mucosal immune responses to determine what constitutes protective immunity to *C. parvum*.

Cryptosporidium parvum is an Apicomplexan sporozoan parasite that has attracted increasing attention as one of the primary causes of diarrhea globally (13, 14, 49, 57). Infection of immunocompetent individuals with *C. parvum* results in flu-like symptoms and profuse watery diarrhea (14, 57). While disease is generally self-limiting in this population, infection of immunocompromised individuals results in protracted illness and diarrhea that can be fatal. Moreover, while infection of immunocompetent individuals remains localized to the gastrointestinal (GI) tract, *C. parvum* can colonize extraintestinal sites in an immunocompromised host (14, 57, 67). Resolution of cryptosporidiosis in immunocompromised individuals is further hampered by the lack of effective chemotherapeutic agents (42). This indicates that immunotherapeutic or combined chemotherapeutic and immunotherapeutic approaches may be necessary for the successful treatment of cryptosporidiosis.

The development of effective vaccines or immunotherapy requires knowledge of the immune mechanisms responsible for the clearance of *C. parvum* from the infected host. However, our current understanding of the immune response to this parasite remains limited. Advances in this area have been significantly impeded by the lack of a suitable murine model of *C. parvum* infection due to the difficulty in inducing an acute, detectable infection in immunocompetent mice 3 weeks of age or older (17, 48). Therefore, most of what is known about the immune response to *C. parvum* is the result of studies performed in neonatal mice or in mice which lack functional T and/or B cells (1, 10, 18, 25, 29, 30, 32–34, 40, 50, 60, 62, 65). Adoptive transfer and antibody depletion studies, as well as experiments completed in major histocompatibility complex class II-deficient mice, have demonstrated the importance of $CD4^+$ T cells and gamma interferon (IFN-γ) during an immune response to *C. parvum* (1, 10, 30, 40, 62). However, the specific subset and function of the $CD4^+$ T cells that are required for protection are unknown. The role of $CD8^+$ T lymphocytes in the resolution of a *C. parvum* infection also remains unresolved, with results ranging from no role to a small but significant contribution (1, 10, 30, 40, 62).

One limitation of the studies discussed above is that the approaches taken do not allow for the detailed characterization of an ongoing immune response that occurs as a consequence of infection. The present study was designed, in part, to determine the ability of mice to resolve a *C. parvum* infection in the complete absence of IFN-γ. This objective was addressed by the use of mice on a C57BL/6 background that have a targeted disruption of the IFN-γ gene (IFN-γ knockout or GKO [15]). IFN-γ knockout mice have proven to be valuable for investigating the ability of this cytokine to mediate protec-

* Corresponding author. Mailing address: Department of Biomedical Sciences, Tufts University School of Veterinary Medicine, 200 Westboro Rd., Building 20-TVDL, North Grafton, MA 01536. Phone: (508) 839-7939. Fax: (508) 839-7977. E-mail: ctheodos@opal.tufts.edu.

† Present address: New England Regional Primate Research Center, Harvard Medical School, Southborough, MA 01772.

tive immunity to pathogenic microorganisms (2, 6, 12, 19, 20, 21, 24, 64). In particular, important information has been provided on the role of IFN-γ in the development of antigen-specific Th1 and Th2 $CD4^+$ T cells (6, 21, 64), $CD8^+$ T cells (21), antibody responses (2, 6, 21), and the involvement of additional cytokines in protective immunity (6, 19) to pathogens as diverse as *Mycobacterium bovis* (20), *Mycobacterium tuberculosis* (12, 19), *Leishmania major* (64), *Listeria monocytogenes* (24), influenza virus type A (21), *Schistosoma mansoni* (2), and herpes simplex virus type 1 (6).

The infection profile in adult immunocompetent C57BL/6J mice following temporary neutralization of IFN-γ activity in vivo was also addressed in our study. Our results indicated that while temporary neutralization of IFN-γ activity enhanced the susceptibility of C57BL/6J mice to infection with *C. parvum*, the mice were ultimately able to clear the parasite from the GI tract. In contrast, this same strain of mouse was unable to resolve a *C. parvum* infection in the complete absence of IFN-γ. In addition to providing insight into the role of IFN-γ during an immune response to *C. parvum*, the use of mice that contain functional B and T lymphocytes offers suitable murine models that allow characterization of the protective immune response to this parasite.

MATERIALS AND METHODS

Mice. A litter of 129/SV × C57BL/6 mice (n7 generation) containing animals homozygous for functional IFN-γ genes (wild type), homozygous for disrupted IFN-γ genes (GKO), and their heterozygous littermates was obtained from Genentech, Inc., South San Francisco, Calif. (15). These mice were 96.9% homologous to the C57BL/6 strain. The GKO mutation was produced as previously described (15). Mice homozygous for this disruption do not produce IFN-γ but have an otherwise fully developed immune system. A mouse colony was generated in-house by repeatedly intercrossing the heterozygous mice, followed by genotypic PCR analysis of genomic DNA isolated from tail snips. Four- to seven-week-old GKO and wild-type mice were used for all of the studies presented here. For the development of our healing model of infection, 4- to 6-week-old C57BL/6J mice were obtained from Jackson Laboratories, Bar Harbor, Maine. All C57BL/6J mice were randomized for body weight prior to the initiation of an experiment. All mice were housed in microisolator cages in approved facilities and were handled according to National Institutes of Health guidelines.

C. parvum. The GCH1 isolate of *C. parvum* used for these studies was originally procured from a patient with AIDS and has been maintained in our laboratory by repeated passage through calves (58). Following collection from infected calves, all feces were homogenized and filtered. The filtered feces were mixed with equal parts of distilled water and 20% ether (final concentration) and centrifuged at 1,100 × *g* for 30 min, followed by two washes at 1,100 × *g* for 15 min in distilled water. The pellet was next layered over a Sheathers discontinuous sucrose gradient and centrifuged at 1,100 × *g* for 30 min, washed twice, and then centrifuged again at 12,000 × *g* for 30 min over a Percoll gradient (9 parts Percoll–1 part 10× Alsever's–9 parts 1× Alsever's; Sigma, St. Louis, Mo.). The purified oocysts were washed twice in distilled water and treated with 1.75% bleach (45) prior to the initiation of infection. For the proliferation assays, bleached oocysts were excysted in vitro by constant shaking for 1 h at 37°C in Leibovitz L-15 medium (GIBCO BRL, Grand Island, N.Y.) containing 0.75% taurocholic acid (Sigma). The excysted sporozoites were separated from the unexcysted oocysts and empty shells by passage through a sterile 2.0-μm-pore-size polycarbonate filter (Costar, Cambridge, Mass.). The purified sporozoites were washed twice with sterile phosphate-buffered saline. The final pellet was resuspended in tissue culture medium, and the sporozoites were counted with a hemocytometer. Sporozoites were used in our in vitro proliferation assays freshly excysted or as a freeze-thaw antigen preparation.

Antibodies. Two hours prior to the initiation of infection, C57BL/6J mice received a single intraperitoneal injection of 1 mg of XMG 1.2, an IFN-γ-neutralizing rat anti-mouse immunoglobulin G1 (IgG1) monoclonal antibody (MAb), kindly provided by Robert Coffman, DNAX Research Institute, Palo Alto, Calif. Each mouse in the control group received a single intraperitoneal injection of 1 mg of normal rat IgG (Sigma).

Infection of mice. All mice were infected via oral inoculation with 10^7 *C. parvum* GCH1 oocysts. The level of oocyst shedding was determined three times per week throughout the course of the study by microscopic observation of 30 high-power fields of a Kinyoun carbol fuchsin-stained fecal smear (59) from each infected animal. Body weights were determined three times per week throughout the course of the study.

Histology. The extent of mucosal infection was determined from randomly selected mice at various time points by histological analysis of multiple intestinal sites (pyloric region of the stomach, six sections from the small intestine, terminal ileum, cecum, proximal colon, and liver/gall bladder) that were fixed in Bouin's fixative (59). Twenty-four hours later, all sections were trimmed, placed in 10% formalin, and processed for histology. The tissue sections were stained with hematoxylin and eosin and blindly examined to determine the extent of infection and pathology.

Proliferation assay. Mesenteric lymph nodes (MLNs) were isolated from infected nonhealing GKO and healing XMG 1.2-treated C57BL/6J mice at 14 and 17 days of infection, respectively. These time points correspond to the terminal (day 14 for GKO mice) and healing (day 17 for XMG 1.2-treated C57BL/6J mice) phases of each model. Single cell suspensions were prepared by passage of the MLNs through a sterile wire mesh. The MLN cells were plated at a concentration of 8×10^5 cells per well in 96-well, flat-bottomed microtiter plates (Costar) and restimulated in vitro with supplemented Dulbecco's modified Eagle medium (GIBCO BRL) containing 0.5% normal mouse serum (8, 53, 54) and various concentrations of freshly excysted *C. parvum* sporozoites or a freeze-thaw sporozoite antigen preparation. To assess the antigenic specificity of the proliferative response, 100 μg of ovalbumin per ml was included in the assay as a parasite-unrelated antigen. Proliferation was determined by the addition of 1 μCi of [^{3}H]thymidine (6.7 Ci/mmol; NEN, Boston, Mass.) to each well 24, 48, or 72 h postinitiation of the in vitro culture. The cells were harvested 24 h after the addition of [^{3}H]thymidine with a cell harvester (Cambridge Technology, Inc., Watertown, Mass.), and the amount of [^{3}H]thymidine incorporated by the cells was determined with a liquid scintillation counter (Beckman, Fullerton, Calif.). Background proliferation was determined by culturing the cells in the absence of antigenic stimulation (culture medium alone). Results are presented as the mean counts per minute of quadruplicate wells stimulated with antigen minus the mean background counts per minute ± standard deviation.

Cytokine ELISAs. Supernatants were harvested from restimulated MLNs at 24, 48, and 72 h postinitiation of the cultures to assess in vitro interleukin 2 (IL-2), IL-4, and IFN-γ production. Cytokine-specific enzyme-linked immunosorbent assays (ELISAs) were performed as previously described (8). Immunoplates (MaxiSorp; Nunc, Roskilde, Denmark) were coated overnight at 4°C with the appropriate capture antibody diluted in 0.1 M $NaHCO_3$ buffer, pH 9.6. All remaining active sites were blocked with phosphate-buffered saline–10% fetal bovine serum (GIBCO BRL) for 2 h at room temperature. Cytokine standards and culture supernatants were added to the wells and incubated overnight at 4°C. Bound cytokines were detected with the appropriate biotinylated anticytokine antibody. The assay was developed with tetramethylbenzidine substrate (Kirkegaard & Perry, Gaithersburg, Md.) and stopped with phosphoric acid (1:20 dilution). For each ELISA, the following reagents were used: for IL-2, capture antibody JES6-1A12 (1 μg/ml; PharMingen, San Diego, Calif.), detecting antibody JES6-5H4 (1 μg/ml; PharMingen), and recombinant murine interleukin 2 (rmuIL-2) (PharMingen); for IL-4, capture antibody 11B11 (2 μg/ml, Biological Response Modifiers Program [BRMP]; National Cancer Institute, Frederick, Md.), detecting antibody BVD6-24G2 (1 μg/ml; PharMingen), and rmuIL-4 (BRMP; National Cancer Institute); and for IFN-γ, capture antibody R46A2 (2 μg/ml; National Institute for Allergy and Infectious Diseases Repository, Braton Biotech, Inc., Rockville, Md.), detecting antibody XMG 1.2 (2 μg/ml; PharMingen), and rmuIFN-γ (PharMingen). These protocols resulted in ELISAs with the following sensitivities: 625 pg/ml for IL-2 and IFN-γ and 250 pg/ml for IL-4.

Statistics. The weights and oocyst shedding (fecal oocysts per 30 high-power fields) of individual mice were analyzed with the Statistical Package for the Social Sciences (SPSS) version 6.1.2 or 7.0 in an OS/2 or Windows 95 environment. For oocyst shedding, data were analyzed with multiple analysis of variance and individual *t* tests as indicated. In general, a two-tailed statistical significance of ≤ 0.05 was considered significant for individual *t* tests, but only after individual group differences were established by analysis of variance testing. All comparisons between groups satisfied not only Student-Newman-Keuls criteria for significant differences but also those of Scheffé's test. For the determination of statistical differences between body weight gain, we performed a pooled analysis of all our experimental data that included the experiments reported herein. Lowess iterative locally weighted least-squares regressions were used to plot trends over time.

RESULTS

Oocyst shedding. The present study was designed in part to examine the profile of *C. parvum* infection in mice containing a disruption in the IFN-γ gene. The following results from one experiment are representative of those from four independent experiments with four to five GKO and two to four female wild-type mice per experiment. We consistently found that GKO mice were exquisitely susceptible to infection with *C. parvum*. While oocyst shedding was generally below detectable levels in infected wild-type mice, the levels of oocyst shedding in infected GKO mice were extremely high (Fig. 1) ($P \leq$

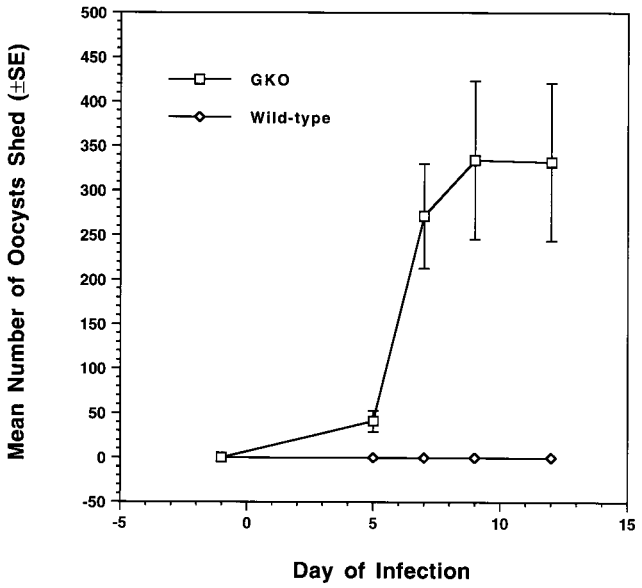

FIG. 1. Oocyst shedding by *C. parvum*-infected female GKO mice and their wild-type littermates. Four to seven-week-old female GKO mice (□, $n = 4$) and their wild-type littermates (◇, $n = 4$) were orally inoculated with 10^7 GCH1 oocysts. Beginning on day 5 of infection, the level of oocysts shed in the feces of each mouse was assessed three times per week by microscopic observation of 30 high-power fields of a Kinyoun carbol fuchsin-stained fecal smear. Results are expressed as the mean number of oocysts shed per group ± standard error (SE).

0.001). These differences in oocyst shedding between GKO and wild-type mice were consistent and statistically powerful, despite the limitations in group size due to our in-house breeding program. Moreover, no difference in susceptibility to infection, as determined by oocyst shedding, was observed between female and male GKO mice (data not shown). Infected GKO mice began shedding oocysts by day 4 to 5 of infection, with peak levels of shedding evident on days 8 to 11 of infection. These mice continued to shed extremely high levels of oocysts throughout the time that they survived. Clinically, the course of disease in GKO mice was rapid, and the animals generally succumbed within 2 to 3 weeks of infection. Preliminary results indicated the same profile of infection and survival time when GKO mice were infected with 10^6 or 10^5 GCH1 oocysts or when n10-generation GKO mice (99.9% homologous to C57BL/6J; Jackson Laboratories) were used (52a).

Experiments were also initiated in this study to determine the infection profile in adult immunocompetent mice following temporary neutralization of IFN-γ activity in vivo. Pretreatment of C57BL/6J mice with a single injection of the neutralizing murine IFN-γ-specific MAb XMG 1.2 significantly enhanced the susceptibility of these mice to infection compared to that of control mice receiving normal rat IgG prior to infection (Fig. 2) ($P \leq 0.001$). The results presented here are reflective of those from three independent experiments with 10 mice per group per experiment. Oocyst shedding was detectable in all XMG 1.2-treated mice by day 5 of infection. Two peaks of shedding were typically observed, with the first peak between days 7 and 10 of infection and the second peak between days 15 and 16 of infection. In contrast to GKO mice, none of the XMG 1.2-treated mice had detectable oocysts in their feces at day 25 of infection. As we observed above with the infected wild-type mice, oocyst shedding was below detectable levels in all normal rat IgG-treated, infected control C57BL/6J mice.

Histological analysis. The GI tracts of uninfected GKO mice were histologically normal, and *C. parvum* parasites were not evident at any time in the infected wild-type mice or in mice heterozygous for the disrupted IFN-γ gene. In contrast, the extent of *C. parvum* infection in the GI tracts of GKO mice at 2 weeks of infection was overwhelming and resulted in profound mucosal destruction (Fig. 3). Moreover, unlike most rodent models, in this model the entire small intestines of GKO mice became infected. We processed and examined six sites from the small intestines of selected GKO mice, and all six were overwhelmingly infected with multiple parasite forms per cell. The villi in the proximal (Fig. 3A) and mid-small intestine (Fig. 3B and D) were contracted, swollen, fused, and infiltrated by inflammatory cells. In addition, some of the crypts in this region were abscessed, displaced, or replaced by fibrous tissue. The mucosa of the distal small intestine was extensively disorganized and edematous, and the lamina propria was heavily infiltrated with inflammatory cells (Fig. 3C). In addition, the crypts were either obliterated or abscessed with fluid, parasite forms, inflammatory cells, and cellular debris. Focal areas of the pyloric region of the stomach were only mildly infected, while the adjacent tissue of the duodenum was heavily infected (data not shown). The cecum and colon were also moderately infected, with a slight alteration in the mucosa, some loss of surface continuity, and goblet cells (data not shown). As with the small intestine, the crypts were either abscessed or absent. In general, the pyloric region of the stomach and the cecum and colon were less extensively infected in this model than in other murine models (1, 40, 59, 60). This was most likely due to the acute nature of the disease. None of the GKO mice displayed signs of hepatobiliary tract infection, which ultimately leads to death in chronically infected SCID

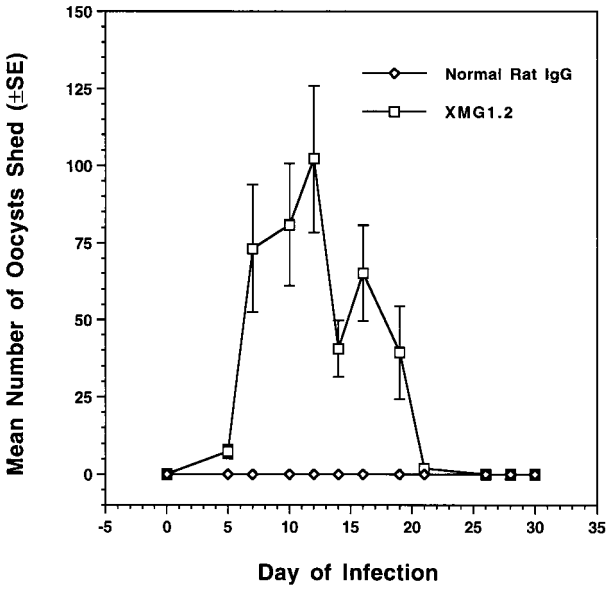

FIG. 2. Oocyst shedding by *C. parvum*-infected C57BL/6J mice. Four to seven-week-old female C57BL/6J mice received a single injection of 1 mg of XMG 1.2 (□, $n = 10$) or normal rat IgG (◇, $n = 10$) 2 h prior to oral inoculation with 10^7 GCH1 oocysts. Beginning on day 5 of infection, the level of oocysts shed in the feces of each mouse was assessed three times per week by microscopic observation of 30 high-power fields of a Kinyoun carbol fuchsin-stained fecal smear. Results are expressed as the mean number of oocysts shed per group ± standard error (SE).

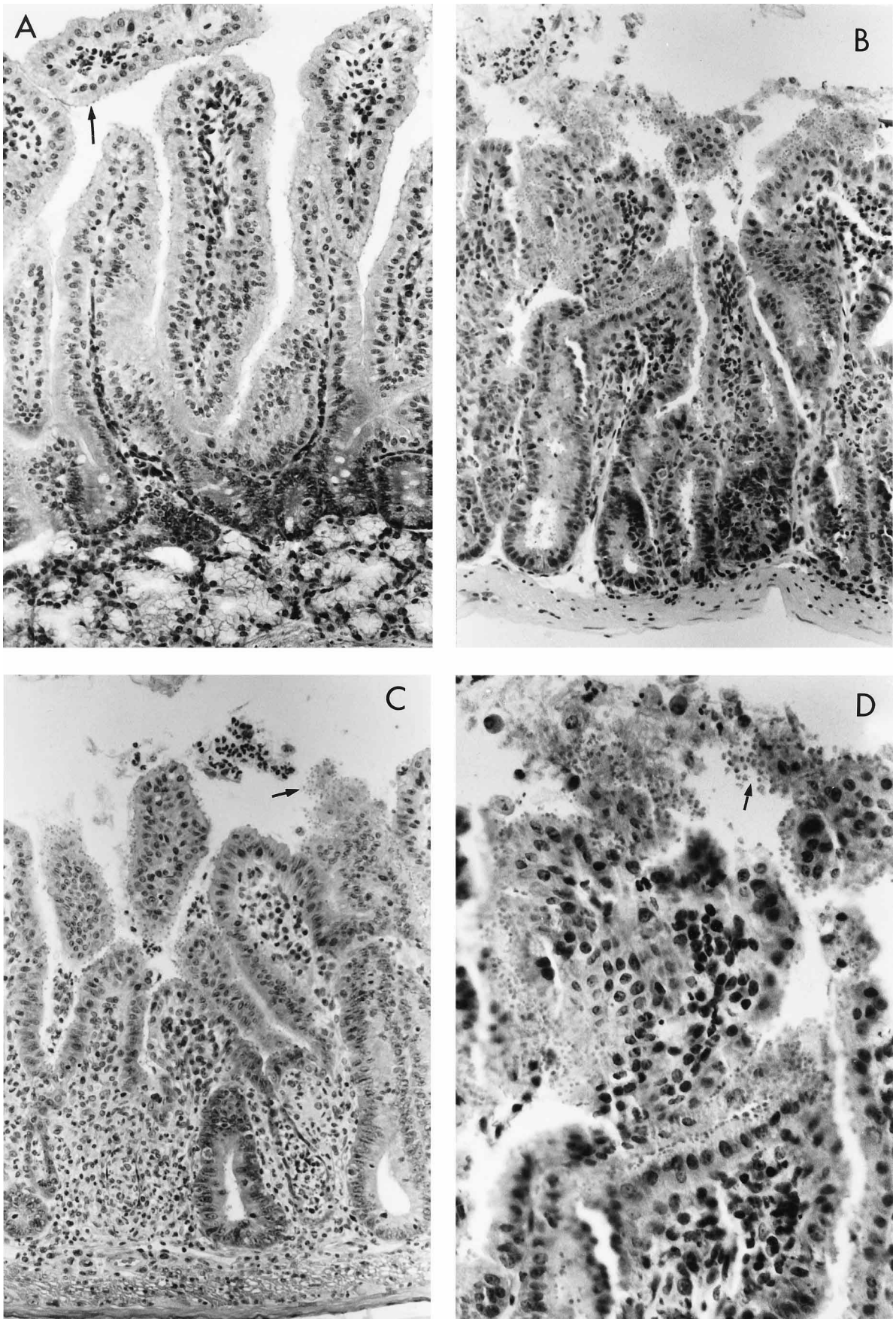
A
B
C
D

FIG. 3. Histological analysis of the proximal (A), mid- (B and D), and distal (C) small intestine of a *C. parvum*-infected GKO mouse, with low (×45 [A to C]) and high (×112 [D]) magnification of hematoxylin-and-eosin-stained sections of the mucosa of the small intestine on day 14 of infection. (A) Slight alteration in the proximal small intestine with shorter, swollen villi and an irregular surface epithelium that is heavily colonized with parasite forms (arrow). (B) Extensive mucosal damage of the mid-small intestine, with severely modified and heavily infected crypts and villus epithelial surfaces. The lamina propria is also moderately infiltrated with inflammatory cells. The extensive infection of the epithelial surface of the mid-small intestine is readily visualized by high-power magnification of this section (arrow, panel D). (C) Extensive alteration in the mucosal architecture of the distal small intestine with a heavy inflammatory cell infiltration. The crypts are either obliterated, fibrotic, or abscessed. The entire mucosal surface is heavily infected (arrow).

mice (32, 33). Instead, the majority of the GKO mice in this study generally succumbed due to a severe acute infection with mucosal destruction of the small intestine.

As in the uninfected GKO mice, the GI tracts of uninfected C57BL/6J mice appeared normal. Histologically, no sign of infection was evident in any of the normal rat IgG-treated, infected control mice. Analysis of the XMG 1.2-treated C57BL/6J mice revealed that, as with the GKO mice, the predominant site of infection was the small intestine. Figure 4 depicts representative results from the mid-small intestine. Although extensive infection and changes in the mucosa were observed in these mice on days 8 (data not shown) and 17 of infection (panels A and B), overall, both were less severe than those observed in infected GKO mice. By 25 days of infection, the extent of parasitization had subsided considerably. The mucosa was free of parasites and appeared essentially normal by 30 days of infection (data not shown). Similar results were observed in the distal small intestine.

Body weight. Weight loss is an additional parameter of severe cryptosporidial infection (25, 33, 59). Analysis of all of our pooled experimental data revealed important differences in weight between the healing and nonhealing models. This pooled data analysis was performed with Lowess iterative locally weighted least-squares regressions of each group over time in order to detect trends in weight loss that would not be statistically evident with the relatively small numbers of mice used in individual experiments. C57BL/6J mice pretreated with a single dose of XMG 1.2 MAb failed to grow during the period of 5 to 15 days after infection (Fig. 5). During this period, their weights were significantly lower than those of mice given normal rat IgG before infection (e.g., at days 5 to 15 after infection, mean ± standard deviation of 17.78 ± 0.09 g for control mice [$n = 115$ observations] versus 16.72 ± 0.10 g for XMG 1.2-treated mice [$n = 249$ observations]; $P < 0.001$). After 15 days, and as the infection began to clear, the XMG 1.2-treated mice demonstrated growth such that by 30 days after infection, their mean weights had increased, although the lag behind the weights of the normal rat IgG-treated control mice was still significant (19.96 ± 0.22 g [$n = 15$] for control mice versus 18.91 ± 0.25 for XMG 1.2-treated mice [$n = 14$]; $P = 0.004$).

In contrast, while wild-type control mice showed normal

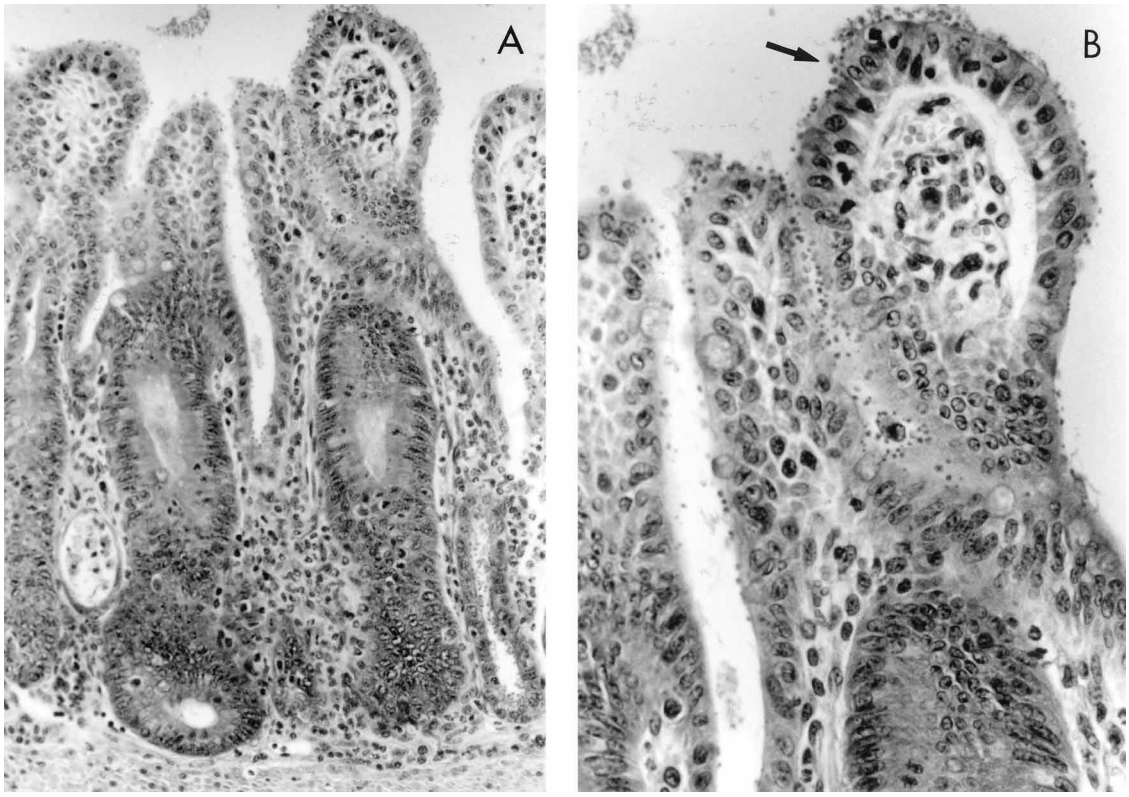

FIG. 4. Histological analysis of the mid-small intestine of a *C. parvum*-infected anti-IFN-γ-treated C57BL/6J mouse, with low (×42 [A]) and high (×105 [B]) magnification of hematoxylin-and-eosin-stained sections of the mid-small intestine taken on day 17 of infection. A representative *C. parvum*-infected C57BL/6J mouse was pretreated with a single injection of the neutralizing anti-IFN-γ MAb XMG 1.2 prior to challenge with *C. parvum*. In panel A, note the moderately altered mucosa with inflammatory cell infiltration, some crypt abscessation, and heavily infected crypt and epithelial cell surfaces. In panel B, note the endogenous parasite stages attached to the epithelial surface (arrow).

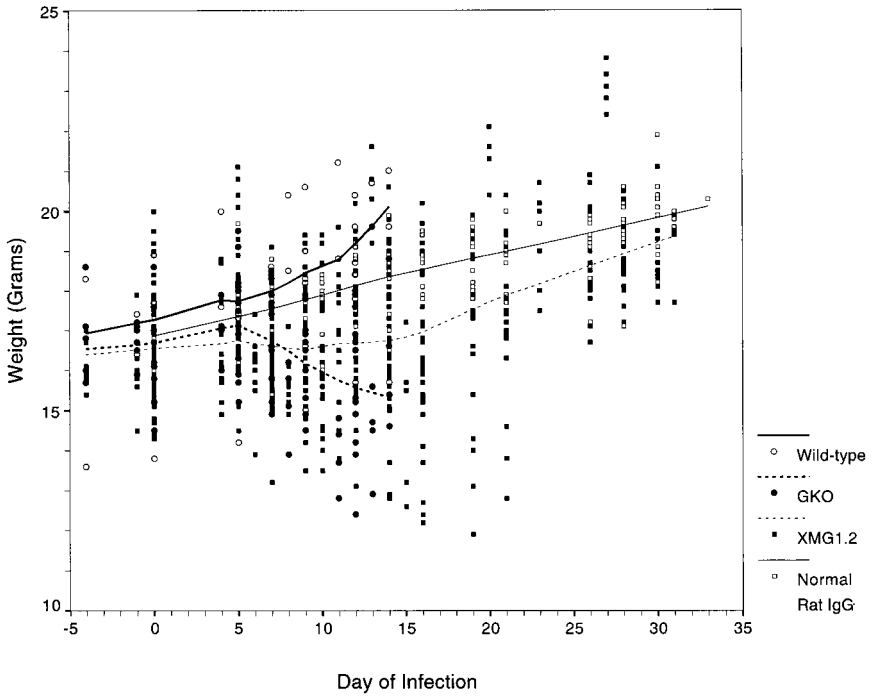

FIG. 5. Body weights of *C. parvum*-infected mice. Shown is a scatter plot of the weights of all *C. parvum*-infected GKO (●), wild-type control (○), XMG 1.2-treated C57BL/6J (■), and normal rat IgG-treated C57BL/6J (□) mice over time. The Lowess iterative locally weighted least-squares regression plots of the weights of each group are displayed.

growth throughout the study, infected GKO mice not only failed to grow but also lost weight rapidly (Fig. 5). Beginning at 5 days after infection, their weights began to decrease, and this pattern continued until the mice had to be euthanized at 2 weeks of infection. This weight loss was significant (days 5 to 15 after infection, 18.48 ± 0.33 g for control wild-type mice [n = 27 observations] versus 15.98 ± 0.22 g for GKO mice [n = 51 observations]; $P < 0.001$).

Proliferative response to *C. parvum*. To ascertain whether a parasite-specific immune response was generated in infected nonhealing GKO and healing XMG 1.2-treated C57BL/6J mice, MLNs were isolated from these mice at 14 and 17 days of infection, respectively. These time points correspond to the terminal (day 14 for GKO mice) and healing (day 17 for XMG 1.2-treated C57BL/6J mice) phases of each model. MLN cells from infected nonhealing GKO (Fig. 6A) and healing C57BL/6J (Fig. 6B) mice proliferated in response to both freshly excysted *C. parvum* sporozoites and the freeze-thaw sporozoite antigen preparation following in vitro restimulation. Analysis of variance revealed significant differences between the proliferative responses induced by the sporozoite antigen preparation and freshly isolated sporozoites ($P < 0.002$ for GKO MLN cells and $P < 0.001$ for C57 MLN cells). Mann-Whitney nonparametric testing of the pooled data indicated that overall, the proliferative response to freshly isolated sporozoites was significantly better than the response to the sporozoite antigen preparation ($P = 0.004$ for MLN cells isolated from both healing C57 and nonhealing GKO mice). Proliferation was not observed following stimulation with ovalbumin, an antigen unrelated to *C. parvum.*

Since *C. parvum* oocysts were isolated from fecal material, it is possible that the proliferative response to sporozoites or the freeze-thaw sporozoite antigen preparation may have been due to residual lipopolysaccharide present in our parasite preparations. To address this issue, we analyzed the proliferative response of MLN cells isolated from *C. parvum*-inoculated wild-type mice and normal rat IgG-treated C57BL/6 mice in which patent infections are undetectable. Following in vitro stimulation with sporozoites or the sporozoite antigen preparation, the proliferative responses of MLN cells from these mice were, on average, 10% to less than 1% of the response observed with MLN cells isolated from infected GKO and anti-IFN-γ-treated C57BL/6 mice. These results suggest that lipopolysaccharide is not a major contributing factor in the parasite-induced proliferative response of MLN cells from nonhealing GKO and healing C57BL/6 mice under the conditions examined.

Cytokine production. MLN cells isolated from *C. parvum*-infected nonhealing GKO and healing C57BL/6J mice secreted IL-2 following restimulation in vitro with freshly excysted sporozoites or a freeze-thaw sporozoite antigen preparation (Table 1). Only MLN cells isolated from healing C57BL/6J mice secreted IFN-γ following restimulation in vitro with *C. parvum*. Analysis of these data by analysis of variance and individual t tests revealed that all cytokine levels were significantly higher than background levels observed following stimulation with medium or ovalbumin ($P < 0.001$). Secretion of IL-4 was not detected in either group at any of the time points examined (i.e., 24-, 48-, and 72-h stimulated cultures).

DISCUSSION

Advances in researchers' understanding of protective immunity to various pathogenic organisms have largely been the result of studies performed with murine models of infection. These models have proven to be extremely useful for studying host antigen-specific immune responses due to their ease of manipulation, existence of genetically inbred strains, and abundant availability of immunological reagents. The studies pre-

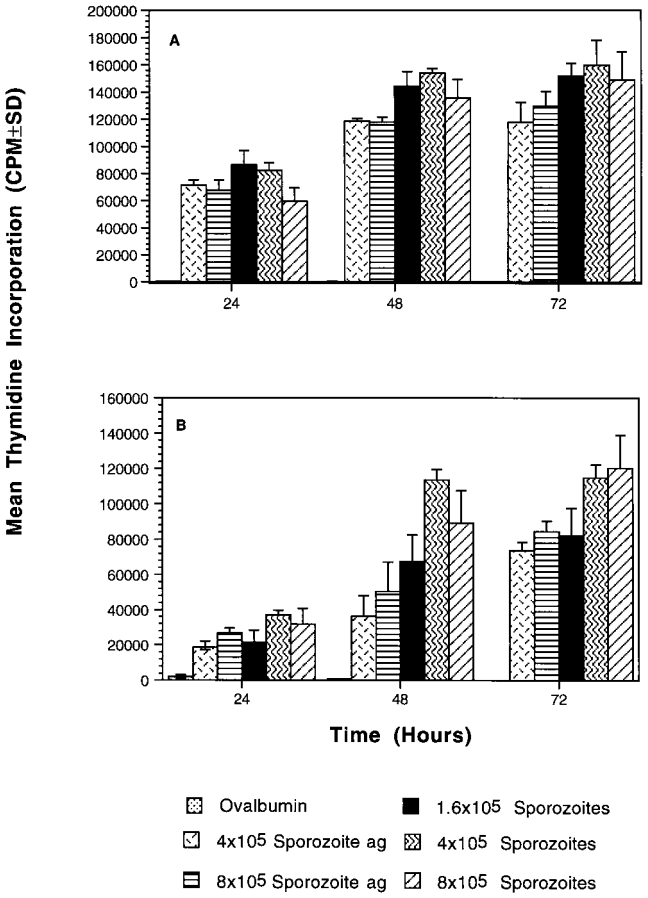

FIG. 6. *C. parvum*-infected GKO and healing C57BL/6J mice mount a parasite-specific immune response. MLNs were isolated from infected nonhealing GKO mice and healing anti-IFN-γ-treated C57BL/6J mice at 14 and 17 days of infection, respectively, and the MLN cells were restimulated in vitro with the indicated stimulus. MLN cells from infected nonhealing GKO (A) and healing C57BL/6J (B) mice proliferated in response to both freshly excysted *C. parvum* sporozoites and the freeze-thaw sporozoite antigen preparation, but not to ovalbumin, a parasite-unrelated antigen.

sented here have characterized healing and nonhealing murine models of *C. parvum* infection that offer several advantages. First, unlike in most other murine models of *C. parvum* infection (25, 29, 32, 33, 59, 60), the entire small intestine was the primary site of infection in both of our models, resulting in an infection profile which closely approximates that seen in animals and humans exhibiting severe clinical infection due to *C. parvum* (14, 57). While diarrhea was not evident in either of our models, a caveat of other murine models as well, the mucoid consistency of the feces from *C. parvum*-infected GKO mice indicated signs of maldigestion and malabsorption, particularly in the terminal phase. The temporary cessation of growth observed in our healing C57BL/6J model, followed by a period of accelerated weight gain during recovery, was similar to what is seen in metabolically stressed children during and after diarrheal diseases (5, 27).

A second advantage of our models is that, unlike other murine models of *C. parvum* infection (1, 10, 25, 29, 30, 32–34, 40, 50, 60, 62, 65), they involve adult mice that have functional T and B lymphocytes. This provides the opportunity for a full evaluation of *C. parvum*-specific T and B cell-mediated immune responses.

A third advantage to our models is that the level of infection achieved was sufficient to generate parasite-specific immune responses, as evidenced by (i) the ability of mice in our healing model to clear their infection and (ii) the parasite-specific proliferative responses obtained following ex vivo restimulation of MLN cells from mice in both models. Reports in the literature have demonstrated a proliferative response to *C. parvum* antigen with spleen cells from immunized mice (22, 51). With respect to infected mice, proliferative responses to *C. parvum* antigen were observed with spleen cells from mice receiving multioral challenges with *C. parvum* (66) and MLN cells from mice challenged at 3 days of age (35). However, proliferative responses to a soluble *C. parvum* antigen were not detected in splenocytes isolated from BALB/c mice infected at 1 week of age (23) or from C57BL/6 mice infected at 6 weeks of age (11). To our knowledge, this is the first demonstration of a *C. parvum*-specific proliferative response of MLN cells isolated from infected adult mice following in vitro restimulation with freshly excysted, intact *C. parvum* sporozoites. Lastly, the fact that *C. parvum*-infected GKO mice mounted a parasite-specific immune response but failed to control their infection indicates that this immune response was not protective. A comparison of the immune responses elicited in our healing and nonhealing models will allow us to determine what constitutes protective immunity to this parasite.

Our results also underscored the importance of IFN-γ in the immune response to *C. parvum* in these murine models of infection. The administration of a single injection of 1 mg of XMG 1.2 prior to infection results in the temporary neutralization of IFN-γ activity. This is due to the short in vivo half-life of this antibody (approximately 3 to 4 days), resulting in clearance of the MAb within 2 to 3 weeks (11a). In our healing model, temporary and, most likely, partial neutralization of IFN-γ activity in vivo was sufficient to render C57BL/6J mice initially susceptible to infection with *C. parvum*. Our result is in accordance with reports in the literature that the administration of an IFN-γ-neutralizing MAb during and/or prior to

TABLE 1. IL-2 and IFN-γ secretion following in vitro restimulation of MLN cells isolated from infected nonhealing GKO and healing C67BL/6J mice

Stimulus	GKO[a]		C67BL/6J[b]	
	IL-2[c]	IFN-γ[c]	IL-2	IFN-γ
Medium	BDL[d]	BDL	BDL	BDL
Ovalbumin	BDL	BDL	BDL	BDL
Antigen[e]				
4×10^5	5.5 ± 1.7	BDL	BDL	10.5 ± 3
8×10^5	4.7 ± 0.8	BDL	2 ± 0.3	23.1 ± 5
1.6×10^6	8.8 ± 4	BDL	1.6 ± 0.06	20.9 ± 4.6
Sporozoites[f]				
1.6×10^5	6.8 ± 0.8	BDL	1.9 ± 0.03	13.4 ± 2.8
4×10^5	10 ± 4.7	BDL	2 ± 0.2	10.6 ± 2.4
8×10^5	11.6 ± 4	BDL	2.3 ± 0.2	8.6 ± 1.4
Concanavalin A	14 ± 3.5	BDL	7.2 ± 3	10.8 ± 2.5

[a] MLNs were harvested on day 14 of infection.
[b] MLNs were harvested on day 17 of infection.
[c] Results are presented as nanograms/milliliter of IL-2 and IFN-γ.
[d] BDL, below detectable limit of the assay.
[e] Number of sporozoite equivalents in a freeze-thaw antigen preparation added per well to the proliferation assay.
[f] Number of freshly excysted sporozoites added per well to the proliferation assay.

infection abrogates the innate resistance of SCID (9, 59) and congenitally athymic nude (62) mice to infection. However, unlike SCID and nude mice, the mice in our healing model were ultimately able to clear the parasite from the GI tract 3 to 4 weeks after infection. Our ex vivo restimulation results suggest that clearance of this parasite correlates with the generation of a *C. parvum*-specific immune response and the secretion of IL-2 and IFN-γ but not of IL-4.

While it is generally agreed that IFN-γ enhances initial resistance to *C. parvum* infection (9, 28, 30, 59, 63), the function of this cytokine in the resolution of infection is unclear. A study by Ungar et al. demonstrated that weekly administration of a neutralizing IFN-γ-specific MAb enhanced the level of oocyst shedding from *C. parvum*-infected, adult BALB/c mice but that the infection was self-limiting (62). Similar results were obtained by McDonald et al. with C57BL/6 and BALB/c mice infected with *Cryptosporidium muris* (29). The authors of each of these studies concluded that the resolution of cryptosporidiosis required IFN-γ-independent effector mechanisms. In contrast is a study by Chen et al. (10), who demonstrated that administration of the neutralizing IFN-γ-specific MAb R46A2 to *C. parvum*-infected SCID mice reconstituted with immunocompetent spleen cells resulted in an abrogation of the resolution of infection imparted by the adoptively transferred cells. One explanation for these conflicting results is that some IFN-γ activity may remain due to incomplete neutralization by the antibody. Our results obtained from *C. parvum*-infected GKO mice are in agreement with those of Chen et al. (10). The ex vivo analysis of parasite-specific MLN cells isolated from infected GKO mice revealed that these cells secreted IL-2 but not IFN-γ or IL-4 in response to *C. parvum*. Collectively, our results from both models suggest that IFN-γ, either directly or indirectly, is important in both the initial resistance to and the resolution of infection in mice on a C57BL/6 background. Moreover, our data to date also suggest that in this system, neither the administration of XMG 1.2 prior to infection nor the absence of IFN-γ resulted in a *C. parvum*-specific immune response skewed toward the production of IL-4, as has been reported for other infectious diseases (6, 47, 64). A complete analysis of the *C. parvum*-specific immune response generated in each of these models is currently being performed in our laboratory to confirm these hypotheses.

Our models could also be used to assess the ability of *C. parvum*-specific Ab responses to protect during an ongoing infection. While all animal species, including humans, produce parasite-specific serum and secretory antibodies in response to *C. parvum* (7, 31, 37, 38, 39, 43, 44), the ability of antibody to mediate protection during an ongoing *C. parvum* infection is unclear. Neonatal BALB/c mice rendered B-cell deficient by anti-μ treatment were still able to clear a *C. parvum* infection (50), and the presence of elevated IgA in the serum of human immunodeficiency virus-infected patients did not correlate with clearance of the parasite from these individuals (26). Finally, treatment of infected animals and humans with *C. parvum*-specific MAbs (3, 4, 41, 45, 52) or hyperimmune bovine colostrum (16, 36, 46, 55, 56, 61) had varying degrees of efficacy in reducing the level of infection.

In conclusion, the studies presented in this report have characterized adult murine models of healing and nonhealing *C. parvum* infection. The mice used in these models contain functional T and B lymphocytes and mount a parasite-specific immune response as a consequence of infection. A comparison of the *C. parvum*-specific mucosal immune responses generated in these healing and nonhealing murine models should help to delineate the precise role of IFN-γ, humoral immunity, and the types of $CD4^+$ T cells and cytokines required for the resolution of infection. These studies should ultimately provide us with critical information pertinent to the development of effective immunotherapeutic approaches that may be necessary to resolve otherwise fatal cryptosporidiosis in patients with AIDS.

ACKNOWLEDGMENTS

We are grateful to Tamara Gull and Jonathan Werner for their technical assistance and to Paul Morin, Richard Titus, and Joe Sypek for critical reading and discussion of the manuscript.

This work was supported by NIH contract NOI-AI-25143 (S.T. and C.M.T.), NIH grant R29-AI-39967 (C.M.T.), and a grant from the Department of Comparative Medicine, Tufts University School of Veterinary Medicine (C.M.T.).

REFERENCES

1. **Aguirre, S. A., P. H. Mason, and L. E. Perryman.** 1994. Susceptibility of major histocompatibility complex (MHC) class I- and class II-deficient mice to *Cryptosporidium parvum* infection. Infect. Immun. **62:**697–699.
2. **Amiri, P., M. Haak-Frendscho, K. Robbins, J. H. McKerrow, T. Stewart, and P. Jardieu.** 1994. Anti-immunoglobulin E treatment decreases worm burden and egg production in *Schistosoma mansoni*-infected normal and interferon gamma knockout mice. J. Exp. Med. **180:**43–51.
3. **Arrowood, M. J., J. R. Mead, J. L. Mahr, and C. R. Sterling.** 1989. Effects of immune colostrum and orally administered antisporozoite monoclonal antibodies on the outcome of *Cryptosporidium parvum* infections in neonatal mice. Infect. Immun. **57:**2283–2288.
4. **Bjorneby, J. M., B. D. Hunsaker, M. W. Riggs, and L. E. Perryman.** 1991. Monoclonal antibody immunotherapy in nude mice persistently infected with *Cryptosporidium parvum*. Infect. Immun. **59:**1172–1176.
5. **Black, B. E., K. H. Brown, and S. Becker.** 1984. Effects of diarrhea associated with specific enteropathogens on the growth of children in rural Bangladesh. Pediatrics **173:**799–805.
6. **Bouley, D. M., S. Kanagat, W. Wire, and B. T. Rouse.** 1995. Characterization of herpes simplex virus type-1 infection and herpetic stromal keratitis development in IFN-γ knockout mice. J. Immunol. **155:**3964–3971.
7. **Campbell, P. N., and W. L. Current.** 1983. Demonstration of serum antibodies to *Cryptosporidium* sp. in normal and immunodeficient humans with confirmed infection. J. Clin. Microbiol. **18:**165–169.
8. **Chakkalath, H. R., C. M. Theodos, J. S. Markowitz, M. J. Grusby, L. H. Glimcher, and R. G. Titus.** 1995. Class II major histocompatibility complex-deficient mice initially control an infection with *L. major* but succumb to the disease. J. Infect. Dis. **171:**1302–1308.
9. **Chen, W., J. A. Harp, A. G. Harmsen, and E. A. Havell.** 1993. Gamma interferon functions in resistance to *Cryptosporidium parvum* infection in severe combined immunodeficient mice. Infect. Immun. **61:**3548–3551.
10. **Chen, W., J. A. Harp, and A. Harmsen.** 1993. Requirements for $CD4^+$ cells and gamma interferon in resolution of established *Cryptosporidium parvum* infection in mice. Infect. Immun. **61:**3928–3932.
11. **Cheng, L., K. R. Rasmussen, M. Healey, and S. Yang.** 1996. Primary and secondary infections with *Cryptosporidium parvum* in immunosuppressed adult mice. Am. J. Trop. Med. Hyg. **55:**324–329.

11a. **Coffman, R.** Personal communication.

12. **Cooper, A. M., D. K. Dalton, T. A. Stewart, J. P. Griffin, D. G. Russell, and I. M. Orme.** 1993. Disseminated tuberculosis in interferon γ gene-disrupted mice. J. Exp. Med. **178:**2243–2247.
13. **Current, W. L., and B. L. Blagburn.** 1991. *Cryptosporidium* and microsporidia: some closing comments. J. Protozool. **38:**244S–245S.
14. **Current, W. L., and L. S. Garcia.** 1991. Cryptosporidiosis. Clin. Microbiol. Rev. **4:**325–358.
15. **Dalton, D. K., S. Pitts-Meek, S. Keshav, I. S. Figari, A. Bradley, and T. Stewart.** 1993. Multiple defects of immune cell function in mice with disrupted interferon-γ genes. Science **259:**1739–1742.
16. **Doyle, P. S., J. Crabb, and C. Petersen.** 1993. Anti-*Cryptosporidium parvum* antibodies inhibit infectivity in vitro and in vivo. Infect. Immun. **61:**4079–4084.
17. **Enriquez, F. J., and C. R. Sterling.** 1991. *Cryptosporidium* infections in inbred strains of mice. J. Protozool. **38:**100S–102S.
18. **Ernest, J. A., B. L. Blagburn, D. S. Lindsay, and W. L. Current.** 1986. Infection dynamics of *Cryptosporidium parvum* (Apicomplexa: *Cryptosporidiae*) in neonatal mice (*Mus musculus*). J. Parasitol. **72:**796–798.
19. **Flynn, J. L., M. M. Goldstein, K. J. Triebold, J. Sypek, S. Wolf, and B. R. Bloom.** 1995. IL-12 increases resistance of BALB/c mice to *Mycobacterium tuberculosis* infection. J. Immunol. **155:**2515–2524.
20. **Flynn, J. L., J. Chan, K. J. Triebold, D. K. Dalton, T. A. Stewart, and B. R. Bloom.** 1993. An essential role for interferon γ in resistance to *Mycobacterium tuberculosis* infection. J. Exp. Med. **178:**2249–2254.
21. **Graham, M. B., D. K. Dalton, D. Giltinan, V. L. Braciale, T. A. Stewart, and T. J. Braciale.** 1993. Response to influenza infection in mice with a targeted disruption in the interferon γ gene. J. Exp. Med. **178:**1725–1732.

22. **Harp, J. A., W. M. Whitmire, and R. Sacco.** 1994. In vitro proliferation and production of gamma interferon by murine CD4$^+$ T cells in response to *Cryptosporidium parvum* antigen. J. Parasitol. **80:**67–72.
23. **Harp, J. A., and R. E. Sacco.** 1996. Development of cellular immune functions in neonatal to weanling mice: relationship to *Cryptosporidium parvum* infection. J. Parasitol. **82:**245–249.
24. **Harty, J. T., and M. J. Bevan.** 1995. Specific immunity to *Listeria monocytogenes* in the absence of IFNγ. Immunity **3:**109–117.
25. **Heine, J. H., W. Moon, and D. B. Woodmansee.** 1984. Persistent *Cryptosporidium* infection in congenitally athymic nude mice. Infect. Immun. **43:**856–859.
26. **Kassa, M., E. Comby, D. Lemeteil, P. Brasseur, and J.-J. Ballet.** 1991. Characterization of anti-*Cryptosporidium* IgA antibodies in sera from immunocompetent individuals and HIV-infected patients. J. Protozool. **38:**179S–180S.
27. **Koster, K. F., C. G. Curlin, K. M. Aziz, and A. Haque.** 1981. Synergistic impact of measles and diarrhoea on nutrition and mortality in Bangladesh. Bull. W. H. O. **59:**901–908.
28. **Kuhls, T. L., D. A. Mosier, V. L. Abrams, D. L. Crawford, and R. A. Greenfield.** 1994. Inability of interferon-gamma and aminoguanidine to alter *Cryptosporidium parvum* infection in mice with severe combined immunodeficiency. J. Parasitol. **80:**480–485.
29. **McDonald, V., R. Deer, S. Uni, M. Iseki, and G. J. Bancroft.** 1992. Immune responses to *Cryptosporidium muris* and *Cryptosporidium parvum* in adult immunocompetent or immunocompromised (nude and SCID) mice. Infect. Immun. **60:**3325–3331.
30. **McDonald, V., and G. Bancroft.** 1994. Mechanisms of innate and acquired resistance to *Cryptosporidium parvum* infection in SCID mice. Parasite Immunol. **16:**315–320.
31. **Mead, J. R., M. J. Arrowood, and C. Sterling.** 1988. Antigens of *Cryptosporidium* sporozoites recognized by immune sera of infected animals and humans. J. Parasitol. **74:**135–143.
32. **Mead, J. R., M. J. Arrowood, R. W. Sidwell, and M. C. Healey.** 1991. Chronic *Cryptosporidium parvum* infections in congenitally immunodeficient SCID and nude mice. J. Infect. Dis. **163:**1297–1304.
33. **Mead, J. R., N. Ilksoy, X. You, Y. Belenkaya, M. Arrowood, M. T. Fallon, and R. Schinazi.** 1994. Infection dynamics and clinical features of cryptosporidiosis in SCID mice. Infect. Immun. **62:**1691–1695.
34. **Mead, J. R., M. J. Arrowood, M. C. Healey, and R. W. Sidwell.** 1991. Cryptosporidial infections in SCID mice reconstituted with human or murine lymphocytes. J. Protozool. **38:**59S–61S.
35. **Moss, D. M., and P. J. Lammie.** 1993. Proliferative responses of lymphocytes from *Cryptosporidium parvum*-exposed mice to two separate antigen fractions from oocysts. Am. J. Trop. Med. Hyg. **49:**393–401.
36. **Nord, J., P. Ma, D. DiJohn, S. Tzipori, and C. O. Tacket.** 1990. Treatment with bovine hyperimmune colostrum of cryptosporidial diarrhea in AIDS patients. AIDS **4:**581–584.
37. **Ortega-Mora, L. M., J. M. Troncoso, F. A. Rojo-Vazquez, and M. Gomez-Bautista.** 1993. Serum antibody response in lambs naturally and experimentally infected with *Cryptosporidium parvum*. Vet. Parasitol. **50:**45–54.
38. **Ortega-Mora, L. M., J. M. Troncoso, F. A. Rojo-Vazquez, and M. Gomez-Bautista.** 1994. Identification of *Cryptosporidium parvum* oocyst/sporozoite antigens recognized by infected and hyperimmune lambs. Vet. Parasitol. **53:**159–166.
39. **Peeters, J. E., I. Villacorta, E. Vanopdenbosch, D. Vandergheynst, M. Naciri, E. Ares-Mazás, and P. Yvoré.** 1992. *Cryptosporidium parvum* in calves: kinetics and immunoblot analysis of specific serum and local antibody responses (immunoglobulin A [IgA], IgG, and IgM) after natural and experimental infections. Infect. Immun. **60:**2309–2316.
40. **Perryman, L. E., P. A. Mason, and C. E. Chrisp.** 1994. Effect of spleen cell populations on resolution of *Cryptosporidium parvum* infection in SCID mice. Infect. Immun. **62:**1474–1477.
41. **Perryman, L. E., and J. M. Bjorneby.** 1991. Immunotherapy of cryptosporidiosis in immunodeficient animal models. J. Protozool. **38:**98S–100S.
42. **Petersen, C.** 1992. Cryptosporidiosis in patients infected with the human immunodeficiency virus. Clin. Infect. Dis. **15:**903–909.
43. **Reperant, J. M., M. Naciri, S. Iochmann, M. Tilley, and D. Bout.** 1994. Major antigens of *Cryptosporidium parvum* recognized by serum antibodies from different infected animal species and man. Vet. Parasitol. **55:**1–13.
44. **Reperant, J.-M., M. Naciri, T. Chardes, and D. T. Bout.** 1992. Immunological characterization of a 17-kDa antigen from *Cryptosporidium parvum* recognized early by mucosal IgA antibodies. FEMS Microbiol. Lett. **99:**7–14.
45. **Riggs, M. W., and L. E. Perryman.** 1987. Infectivity and neutralization of *Cryptosporidium parvum* sporozoites. Infect. Immun. **55:**2081–2087.
46. **Riggs, M. W., V. A. Cama, H. L. Leary, Jr., and C. R. Sterling.** 1994. Bovine antibody against *Cryptosporidium parvum* elicits a circumsporozoite precipitate-like reaction and has immunotherapeutic effect against persistent cryptosporidiosis in SCID mice. Infect. Immun. **62:**1927–1939.
47. **Scott, P.** 1991. IFN-γ modulates the early development of Th1 and Th2 responses in a murine model of cutaneous leishmaniasis. J. Immunol. **147:**3149–3155.
48. **Sherwood, D., K. W. Angus, D. R. Snodgrass, and S. Tzipori.** 1982. Experimental cryptosporidiosis in laboratory mice. Infect. Immun. **38:**471–475.
49. **Soave, R.** 1990. Human coccidial infections: cryptosporidiosis and isosporiasis, p. 352–358. *In* K. Warren and A. Mahmoud (ed.), Tropical and geographical medicine, 2nd ed. McGraw-Hill, Inc., New York, N.Y.
50. **Taghi-Kilani, R., L. Sekla, and K. T. Hayglass.** 1990. The role of humoral immunity in *Cryptosporidium* spp. infection. Studies in B cell-depleted mice. J. Immunol. **145:**1571–1576.
51. **Tatalick, L. M., and L. E. Perryman.** 1995. Effect of surface antigen-1 (SA-1) immune lymphocyte subsets and naive cell subsets in protecting *scid* mice from initial and persistent infection with *Cryptosporidium parvum*. Vet. Immunol. Immunopathol. **47:**43–55.
52. **Tatalick, L. M., and L. E. Perryman.** 1995. Attempts to protect severe combined immunodeficient (scid) mice with antibody enriched for reactivity to *Cryptosporidium parvum* surface antigen-1. Vet. Parasitol. **58:**281–290.

52a. **Theodos, C.** Unpublished observation.

53. **Theodos, C. M., and R. G. Titus.** 1993. Salivary gland material from the sand fly *Lutzomyia longipalpis* has an inhibitory effect on macrophage function *in vitro*. Parasite Immunol. **15:**481–487.
54. **Titus, R. G., G. Lima, H. D. Engers, and J. A. Louis.** 1984. Exacerbation of murine cutaneous leishmaniasis by adoptive transfer of parasite-specific helper T cell populations capable of mediating *Leishmania major*-specific delayed-type hypersensitivity. J. Immunol. **133:**1594–1600.
55. **Tzipori, S., D. Robertson, and C. Chapman.** 1986. Remission of diarrhoea due to cryptosporidiosis in an immunodeficient child treated with hyperimmune bovine colostrum. Br. Med. J. **293:**1276–1277.
56. **Tzipori, S., D. Robertson, D. A. Cooper, and L. White.** 1987. Chronic cryptosporidial diarrhoea and hyperimmune bovine colostrum. Lancet **ii:**344–345.
57. **Tzipori, S.** 1988. Cryptosporidiosis in perspective. Adv. Parasitol. **27:**63–129.
58. **Tzipori, S., W. Rand, J. Griffiths, G. Widmer, and J. Crabb.** 1994. Evaluation of an animal model system for cryptosporidiosis: therapeutic efficacy of paromomycin and hyperimmune bovine colostrum-immunoglobulin. Clin. Diagn. Lab. Immunol. **1:**450–463.
59. **Tzipori, S., W. Rand, and C. M. Theodos.** 1995. Evaluation of a two-phase *scid* model preconditioned with anti-interferon-γ monoclonal antibody for drug testing against *Cryptosporidium parvum*. J. Infect. Dis. **172:**1160–1164.
60. **Ungar, B. L. P., J. A. Burris, C. A. Quinn, and F. D. Finkelman.** 1990. New mouse models for chronic *Cryptosporidium* infection in immunodeficient hosts. Infect. Immun. **58:**961–969.
61. **Ungar, B. L. P., D. J. Ward, R. Fayer, and C. A. Quinn.** 1990. Cessation of *Cryptosporidium*-associated diarrhea in an acquired immune deficiency syndrome patient after treatment with hyperimmune bovine colostrum. Gastroenterology **98:**486–489.
62. **Ungar, B. L. P., T.-Z. Kao, J. A. Burris, and F. D. Finkelman.** 1991. *Cryptosporidium* infection in an adult mouse model. Independent roles for IFN-γ and CD4$^+$ T lymphocytes in protective immunity. J. Immunol. **147:**1014–1022.
63. **Urban, J. F., R. Fayer, S.-J. Chen, W. C. Gause, M. K. Gately, and F. Finkelman.** 1996. IL-12 protects immunocompetent and immunodeficient neonatal mice against infection with *Cryptosporidium parvum*. J. Immunol. **156:**263–268.
64. **Wang, Z.-E., S. L. Reiner, S. Zheng, D. K. Dalton, and R. M. Locksley.** 1994. CD4$^+$ effector cells default to the TH2 pathway in interferon γ-deficient mice with *Leishmania major*. J. Exp. Med. **179:**1367–1371.
65. **Waters, W. R., and J. A. Harp.** 1996. *Cryptosporidium parvum* infection in T-cell receptor (TCR)-α- and TCR-γ-deficient mice. Infect. Immun. **64:**1854–1857.
66. **Whitmire, W., and J. Harp.** 1990. In vitro murine lymphocyte blastogenic responses to *Cryptosporidium parvum*. J. Parasitol. **76:**450–452.
67. **Wilson, M.** 1991. A world guide to infectious diseases, distribution and diagnosis, p. 476–477. Oxford University Press, Inc., New York, N.Y.

Editor: R. E. McCallum